Synthesis of (*E*)-5-(2-arylvinyl)-2-(hetero)arylpyridines, (*E*)-2-(2-arylvinyl)-5-methoxycarbonylpyridines and (*E*,*E*)-2,5-bis(2-arylvinyl)pyridines as polarity and pH probes †

Erik Van der Eycken,*[a] Zhang Jidong,[a] Amuri Kilonda,[a] Frans Compernolle,[a] Suzanne Toppet,[a] Georges Hoornaert,[a] Mark Van der Auweraer,*[b] Carine Jackers,[b] Wouter Verbouwe[b] and Frans C. De Schryver[b]

[a] *Laboratory for Organic Synthesis, K.U.Leuven, Department of Chemistry, Celestijnenlaan 200 F, B-3001 Heverlee, Belgium*
[b] *Laboratory for Molecular Dynamics and Spectroscopy, K.U.Leuven, Department of Chemistry, Celestijnenlaan 200 F, B-3001 Heverlee, Belgium*

Received (in Cambridge, UK) 11th January 2002, Accepted 18th March 2002
First published as an Advance Article on the web 11th April 2002

In this report we describe the synthesis and photophysical properties of various (*E*)-5-(2-arylvinyl)-2-(hetero)-arylpyridines **7a**–**f**, (*E*)-2-(2-arylvinyl)-5-methoxycarbonylpyridines **14a**,**b** and (*E*,*E*)-2,5-bis(2-arylvinyl)pyridines **13a**,**b**. The fluorescence spectra and the fluorescence quantum yields of these versatile molecules depend strongly on the polarity and proton donor character of the environment. While the smaller excited state dipole moment of the (*E*)-2-(2-arylvinyl)-5-methoxycarbonylpyridines **14a**,**b** leads to a smaller polarity dependence, the fluorescence of these molecules is characterized by a larger dependence on the proton donor character of the environment. On the other hand, the fluorescence maximum of the (*E*,*E*)-2,5-bis(2-arylvinyl)pyridines **13a**,**b** shows an extremely large dependence on the solvent polarity, but, until salt formation occurs, the proton donor character of the environment hardly influences the fluorescence maximum. The combination of the complementary photophysical properties of both molecules and the synthetic accessibility of derivatives with a large variety of substituents, allowing selective incorporation in various environments, makes them an interesting class of probes.

Introduction

The high sensitivity of fluorescence has prompted the use of fluorescent molecules[1–10] to probe the polarity and acidity[1–17] of the environment in biological[18] as well as synthetic systems. It was the aim of this research to develop probes with a large fluorescence quantum yield, absorbing in the visible and showing a large dependence of the fluorescence quantum yield or emission maximum on the polarity or acidity of the environment. The development of synthetic pathways leading to substituted pyridines allows one to obtain molecules that combine high solvatochromism with a flexible substitution pattern. The latter opens the way to the incorporation of moieties (*e.g.* hydrophobic alkyl groups) leading to a localization of the probes in colloidal regions of biological systems.[8,9,12] In this contribution we want to report on the synthesis of the chromophores and their photophysical properties in low viscosity solvents covering a broad range of polarity and proton donor character.[14,16,17] As the probes are insoluble in water the effect of the addition of acids or bases on their photophysical properties are determined in methanol.

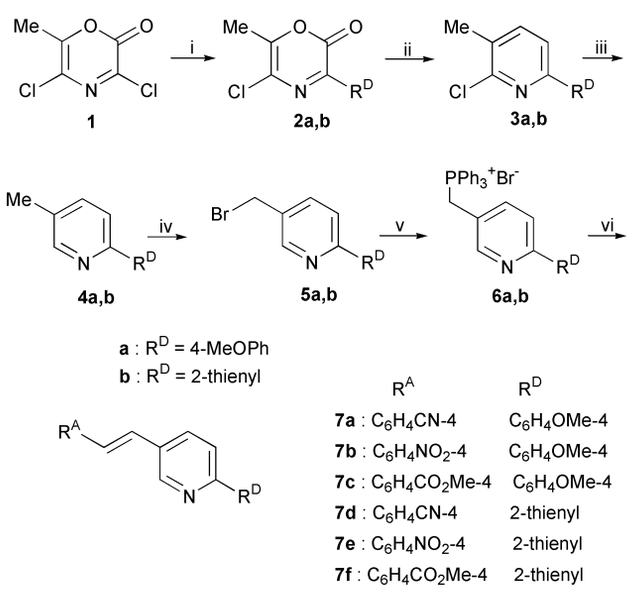

Scheme 1 i) for **a**: 4-MeOPh, $AlCl_3$, CH_2Cl_2, 2 h; for **b**: thiophene, $SnCl_4$, CH_2Cl_2, 12h; ii) bicyclo[2.2.1]hepta-2,5-diene, $CHCl_3$, reflux, 12 h, then pyrolysis at 140 °C; iii) Pd–C (10 %), K_2CO_3, MeOH–THF (1 : 1), H_2 (1 atm), 3 h; iv) NBS, $(PhCO)_2O_2$, CCl_4, reflux, 20 min; v) PPh_3, xylene, reflux, 24 h; vi) 4-substituted benzaldehyde R^ACHO, KOt-Bu, THF, reflux, 24 h.

Results

Synthesis

Two synthetic strategies were used to obtain the fluorescent pyridine derivatives. In the first sequence (Scheme 1) we relied upon our well known 'oxazinone chemistry'.[19] The synthesis of the 3-(hetero)aryl-substituted oxazinones **2a**,**b** has been described previously.[19g] The (*E*)-5-(2-arylvinyl)-2-(hetero)-arylpyridines **7a**–**f** were prepared starting from 3,5-dichloro-6-methyl-2*H*-1,4-oxazin-2-one (**1**). In the second approach (*E*,*E*)-2,5-bis(2-arylvinyl)pyridines **13a**,**b** and (*E*)-2-(2-aryl-

† Electronic supplementary information (ESI) available: details of syntheses and spectroscopic data. See http://www.rsc.org/suppdata/p2/b2/b200446c/

 DOI: 10.1039/b200446c

vinyl)-5-methoxycarbonylpyridines **14a**,**b** were derived from commercially available methyl 6-methylnicotinate (**8**) using a five-step sequence.

(*E*)-5-(2-Arylvinyl)-2-(hetero)arylpyridines 7a–f. Our first synthetic approach (Scheme 1) started with substitution of the reactive 3-chloro position of 3,5-dichloro-6-methyl-2*H*-1,4-oxazin-2-one (**1**) with anisole or thiophene using a suitable Lewis acid catalyst. As previously described,[20] this reaction proceeds *via* an addition–elimination process producing the 3-(hetero)aryl-substituted oxazinones **2a**,**b**. Conversion of **2a**,**b** to the corresponding 6-(hetero)aryl-2-chloro-3-methylpyridines **3a**,**b** was accomplished in excellent yield by reaction with 3 equivalents of bicyclo[2.2.1]hepta-2,5-diene—serving as a precursor to the required but poorly reactive acetylene dienophile—in chloroform at reflux temperature. By thermolysis of the intermediate bridged adducts at 140 °C in a sealed tube two consecutive cycloreversion reactions occur to form the pyridines **3a**,**b**: loss of cyclopentadiene followed by expulsion of carbon dioxide.

Dechlorination of **3a**,**b** to form the corresponding 2-(hetero)-aryl-5-methylpyridines **4a**,**b** was effected by hydrogenation at 1 atm in methanol–THF using Pd on activated carbon as catalyst and K_2CO_3 to capture the liberated HCl.[21] The use of a nickel or a platinum catalyst was unsatisfactory due to the poisoning effect by organic halides of the former[22] and the tendency for overreduction of the latter[23] catalyst. Compounds **4a**,**b** were brominated specifically in their azabenzylic 5-methyl position *via* reaction with NBS in the presence of a peroxide in the nonpolar solvent carbon tetrachloride.[24–26] The 2-(hetero)aryl-5-bromomethylpyridines **5a**,**b** were treated with triphenylphosphine in boiling xylene for 24 hours to produce their phosphonium salts **6a**,**b** in almost quantitative yield. The corresponding ylides were generated and subjected to Wittig olefination under the usual conditions to obtain the (*E*)-configuration[27] (KOt-Bu, THF, reflux) with three substituted benzaldehydes containing an electron-withdrawing group in the *para*-position (4-nitrobenzaldehyde, 4-cyanobenzaldehyde and methyl 4-formylbenzoate). The ^{1}H-NMR spectra of all six 5-(2-arylvinyl)-2-(hetero)arylpyridine products **7a**–**f** revealed a large vicinal coupling constant (14 to 16 Hz) for the two vinylic protons supporting the (*E*)-configuration for the double bond.

(*E*,*E*)-2,5-Bis(2-arylvinyl)pyridines 13a,b and (*E*)-2-(2-arylvinyl)-5-methoxycarbonylpyridines 14a,b. (*E*,*E*)-2,5-Bis(2-arylvinyl)pyridines **13a**,**b** (Scheme 2) were prepared from commercially available methyl 6-methylnicotinate (**8**) using a five-step synthesis. The starting material **8** was reduced with $LiAlH_4$ to give the primary alcohol **9** that was converted to the corresponding chloride **10** upon treatment with thionyl chloride. Subsequent reaction with PPh_3 afforded phosphonium salt **11**. All of these reactions were accomplished with excellent yields (≥90%). The Wittig reaction of **11** with methyl 4-formylbenzoate again was carried out in THF to give exclusively the (*E*)-5-stilbazole product **12** in good yield.[27] This was condensed with 4-(*N*,*N*-dimethylamino)- and 4-methoxybenzaldehyde under Knoevenagel reaction conditions using catalytic amounts of piperidine and acetic acid. The desired compounds, (*E*,*E*)-2,5-bis(2-arylvinyl)pyridines **13a**,**b**, were produced in a fair yield together with the corresponding (*Z*)-2 isomers, which could be removed by crystallisation. This Knoevenagel condensation also was applied directly to methyl 6-methylnicotinate **8** and the same aryl aldehydes to form the (*E*)-2-stilbazoles **14a**,**b**. The (*E*,*E*)-2,5-bis(2-arylvinyl)pyridines **13a**,**b** could also be generated starting from the (*E*)-2-(2-arylvinyl)-5-methoxycarbonylpyridines **14a**,**b**. However, the poor solubility of these compounds renders the subsequent reactions difficult. The structures of **13a**,**b** and **14a**,**b** were confirmed spectroscopically.

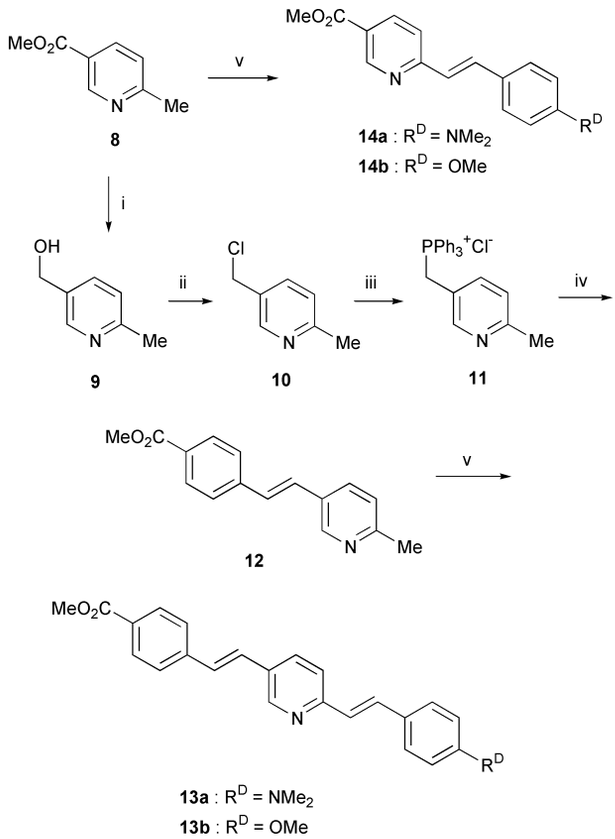

Scheme 2 i) $LiAlH_4$, Et_2O, reflux, 3 h; ii) $SOCl_2$, toluene, reflux, 40 min; iii) PPh_3, xylene, reflux, 20 h; iv) methyl 4-formylbenzoate, KOt-Bu, THF, reflux, 12 h; v) 4-(*N*,*N*-dimethylamino)benzaldehyde or 4-methoxybenzaldehyde, piperidine (catalytic), HOAc (catalytic), toluene, reflux, 3 days.

Photophysical properties

Dependence of the photophysical properties upon the molecular structure and solvent polarity. To investigate to what extent the donor–acceptor character was sufficient to allow the formation of a polar excited state,[28–33] necessary to use the compounds **7**, **14** and **13** as polarity indicators, the absorption and fluorescence spectra in toluene and acetonitrile, as well as the fluorescence quantum yields in toluene and acetonitrile, were obtained (Table 1).

For all compounds a relatively large Stokes shift is observed which does not increase much from toluene to acetonitrile (except for **14a** and **13a**). Apparently, the formation of the polar excited state requires the presence of a dimethylaniline donor moiety. The large Stokes shift in the absence of the formation of the highly polar excited state is probably due to a geometric relaxation of the arylvinyl moieties to a more planar configuration.[28,34–36] Although compounds **7a** and **7d** are characterized by a superior quantum yield, they are not useful as solvent polarity indicators as the emission maximum shifts only 30 nm between toluene and acetonitrile.

For compounds **14a** and **13a** the solvent dependence of the absorption and fluorescence spectra was investigated more extensively (Table 2, Figs. 1–4). The combination of the optical densities (up to 1 in the absorption spectra and up to 0.2 in the emission spectra with the molar absorption coefficient (always larger than 10^4 M^{-1}) gives maximum concentrations of 1×10^{-4} and 2×10^{-5} M. The excitation spectra obtained for the more dilute solutions correspond to the absorption spectra obtained for the more concentrated solutions. Furthermore, there are no changes in the absorption and emission spectra between the different solvents, which cannot be explained by changes in the solvent permanent dipole moment or polarizability. Both sets of data indicate that for the solvents and concentration range studied aggregation is highly unlikely.

Table 1 Spectroscopic properties of (*E*)-5-(2-arylvinyl)-2-(hetero)arylpyridines **7** and (*E*)-2-(2-arylvinyl)-5-methoxycarbonylpyridines **14** and (*E*,*E*)-2,5-bis(2-arylvinyl)-2-(hetero)arylpyridines **13**

Product	**7a**	**7d**	**14a**	**14b**	**13a**	**13b**
$\tilde{\nu}_{tol}^{abs\,a}$/nm	353	360	400	349	418	375
$\varepsilon_{tol}^{abs\,b}$/cm^{-1} M^{-1}	32580	30270	25440	39670	29800	37550
$\tilde{\nu}_{tol}^{flu\,c}$/nm	420[g,h]	422[g,h]	480	419[g,i]	522	445[g,j]
φ_{tol}^{flu}	0.66 ± 0.12	0.50 ± 0.10	0.026 ± 0.005	0.006 ± 0.002	0.53 ± 0.11	0.30 ± 0.06
$\tilde{\nu}_{mcn}^{abs\,d}$/nm	346	348	400	341	404	370
$\varepsilon_{mcn}^{abs\,e}$/cm^{-1}M^{-1}	36230	36810	27730	19950	12050	34180
$\tilde{\nu}_{mcn}^{flu\,f}$/nm	458	435	554	450	638	493
φ_{mcn}^{flu}			0.10 ± 0.02		0.081 ± 0.016	0.42 ± 0.08

[a] Absorption maximum in toluene. [b] Absorption coefficient at the maximum in toluene. [c] Fluorescence maximum in toluene. [d] Absorption maximum in acetonitrile. [e] Absorption coefficient at the maximum in acetonitrile. [f] Fluorescence maximum in acetonitrile. [g] 0⟶1 transition. [h] 0⟶0 transition at 406 nm. [i] 0⟶0 transition at 404 nm. [j] 0⟶0 transition at 433 nm.

Table 2 Solvent dependence of the absorption and fluorescent properties of **14a** and **13a**

	14a			**13a**			ε_r[c]	n[d]
	$\tilde{\nu}_{max}^{abs\,a}$/nm	$\tilde{\nu}_{max}^{flu\,b}$/nm	φ_f	$\tilde{\nu}_{max}^{abs\,a}$/nm	$\tilde{\nu}_{max}^{flu\,b}$/nm	φ_f		
Nonpolarisable, non-proton-donating solvents								
Isooctane	390	454[f](435[h])	0.029 ± 0.006	—[g]	486[f](458[h])		1.94	1.39
Triethylamine	395	483	0.045 ± 0.009	—[g]	—[g]		2.42	1.40
Dibutyl ether	396	479		—[g]	517		3.08	1.40
Diisopropyl ether	389	477		406	520		3.88	1.37
Diethyl ether	395	490	0.063 ± 0.012	402	537	0.24 ± 0.05	4.34	1.35
Butyl acetate	396	510		407	559		5.01	1.39
Ethyl acetate	395	512		410	570		6.02	1.37
THF[e]	400	514	0.129 ± 0.026	412	578	0.50 ± 0.10	7.58	1.40
Butyronitrile	402	537		409	618		20.3	1.38
Acetone	400	540	0.24 ± 0.05	407	628	0.36 ± 0.07	20.0	1.36
Propionitrile	400	545	0.24 ± 0.05	410	627		27.2	1.37
Acetonitrile	400	554	0.28 ± 0.06	404	638	0.081 ± 0.016	37.5	1.34
Dimethyl sulfoxide	413	568	0.30 ± 0.06	422	660	0.09 ± 0.02	46.9	1.48
DMF	405	558	0.27 ± 0.06	415	645	0.16 ± 0.03	36.7	1.43
Polarizable solvents								
Toluene	400	480	0.036 ± 0.007	415	510	0.53 ± 0.11	2.28	1.49
Pyridine	410	545	0.22 ± 0.05	422	623	0.34 ± 0.07	13.1	1.54
Proton-donating solvents								
Acetic acid	485 (430)[g]	610	0.023 ± 0.005	485	620	0.11 ± 0.02	6.15	1.37
Benzyl alcohol	423	565	0.16 ± 0.03	429	615	0.21 ± 0.04	1.01	1.54
Ethanol		568		406	610	0.10 ± 0.02	24.6	1.36
Methanol	406	579	0.23 ± 0.05	411	639	0.043 ± 0.008	32.7	1.33
2,2,2-Trifluoroethanol	385	587	0.032 ± 0.006	379	625	0.030 ± 0.006	26.5	1.29
Formamide	410	588	0.20 ± 0.05	—[g]			111.0	1.45

[a] Absorption maximum. [b] Emission maximum. [c] Relative permittivity. [d] Refractive index. [e] Tetrahydrofuran. [f] Maximum of the 0⟶1 vibronic transition. [g] Insufficiently soluble. [h] 0⟶0 transition.

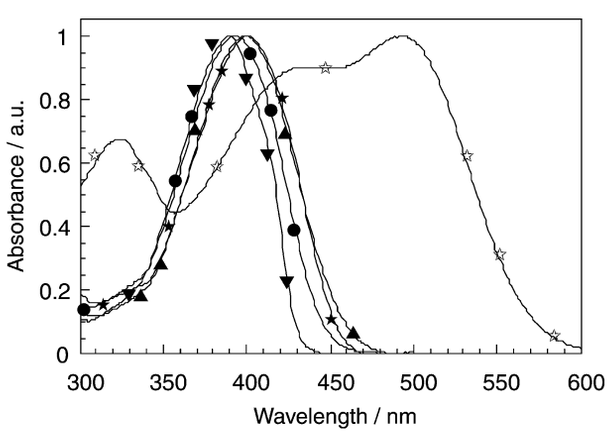

Fig. 1 Absorption spectra of **14a** normalized to one at the maximum; ▼: isooctane, ●: diethyl ether, ▲: acetonitrile, ★: toluene, ☆: acetic acid. The concentration was between 10^{-4} and 2×10^{-5} M.

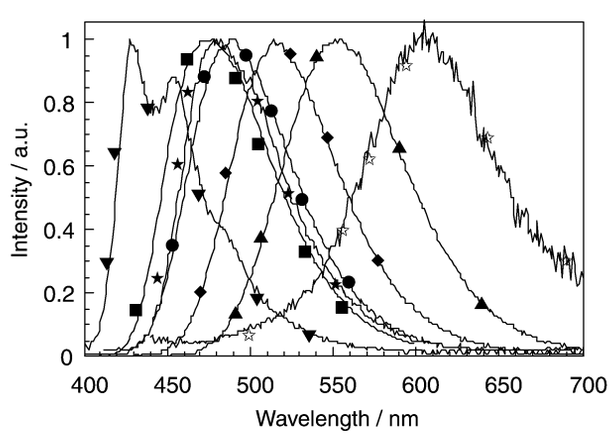

Fig. 2 Fluorescence spectra of **14a** normalized at the maximum; ▼: isooctane, ■: dibutyl ether, ●: diethyl ether, ◆: tetrahydrofuran, ▲: acetonitrile, ★: toluene, ☆: acetic acid. Excitation occurred at 400 nm. The concentration was between 10^{-5} and 5×10^{-6} M.

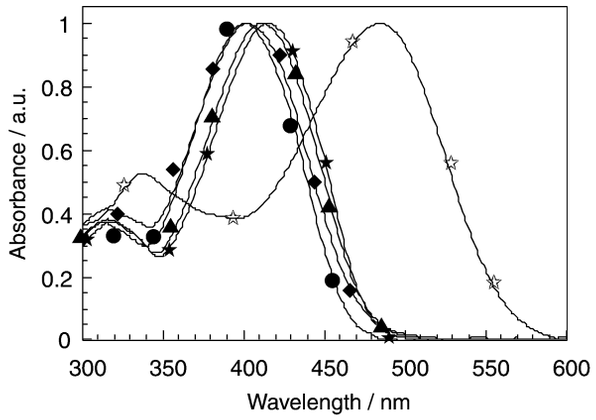

Fig. 3 Absorption spectra of **13a** normalized to one at the maximum; ●: diethyl ether, ◆: tetrahydrofuran, ▲: acetonitrile, ★: toluene, ☆: acetic acid. The concentration was between 10^{-4} and 2×10^{-5} M.

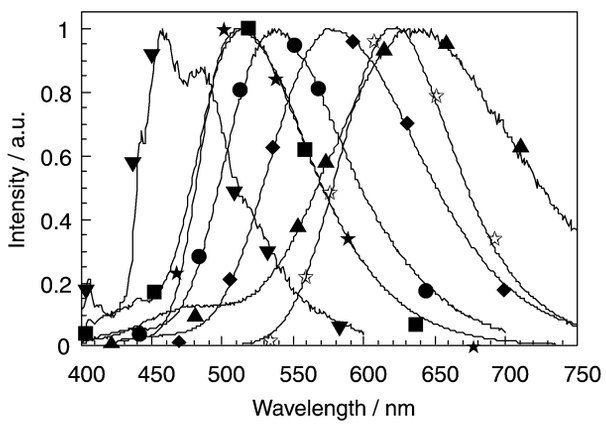

Fig. 4 Fluorescence spectra of **13a** normalized at the maximum; ▼: isooctane, ■: dibutyl ether, ●: diethyl ether, ◆: tetrahydrofuran, ▲: acetonitrile, ★: toluene, ☆: acetic acid. Excitation occurred at 400 nm. The concentration was between 10^{-5} and 5×10^{-6} M.

The large bathochromic shift of the fluorescence of **14a** and **13a** suggests that for both molecules the fluorescent state is highly polar. To the extent that the solute–solvent interactions are limited to dipole–dipole interactions, the solvent dependence of the fluorescence maximum can be derived as follows [10,37,38]

$$\bar{\nu}_f - \bar{\nu}_f^0 = \frac{2(\mu_G - \mu_E)}{4\pi\varepsilon_0 hc\rho^3}\left[\frac{\mu_E(\varepsilon_r - 1)}{2\varepsilon_r + 1} - \frac{(\mu_E - \mu_G)(n^2 - 1)}{2(2n^2 + 1)}\right] \quad (1)$$

where $\bar{\nu}_f$ and $\bar{\nu}_f^0$ correspond to the emission maximum (cm^{-1}) in a solvent with relative permittivity ε_r and refractive index n and the emission frequency *in vacuo* respectively. ε_0, h, c and ρ correspond to the permittivity of vacuum (8.85×10^{-12} C V^{-1} m^{-1}), Planck's constant (6.6×10^{-34} J s), the velocity of light *in vacuo* (3.0×10^{10} cm s^{-1}) and the radius of the solvent cavity (in m). μ_E (C m) and μ_G (C m) are the permanent dipole moments of the ground state and the excited state, respectively.

An analogous expression can be derived for the absorption maximum [10,37,38]

$$\bar{\nu}_{abs} - \bar{\nu}_{abs}^0 = \frac{2(\mu_G - \mu_E)}{4\pi\varepsilon_0 hc\rho^3}\left[\frac{\mu_G(\varepsilon_r - 1)}{2\varepsilon_r + 1} - \frac{(\mu_G - \mu_E)(n^2 - 1)}{2(2n^2 + 1)}\right] \quad (2)$$

where $\bar{\nu}_a$ and $\bar{\nu}_a^0$ correspond to the emission maximum (cm^{-1}) in a solvent with relative permittivity ε_r and refractive index n and the emission frequency *in vacuo*, respectively. This leads to following expression for the Stokes shift $\bar{\nu}_a - \bar{\nu}_f$:

$$\bar{\nu}_{abs} - \bar{\nu}_f = \bar{\nu}_{abs}^0 - \bar{\nu}_f^0 + \frac{2}{4\pi\varepsilon_0 hc\rho^3}\left[\frac{\varepsilon_r - 1}{2\varepsilon_r + 1} - \frac{n^2 - 1}{2(2n^2 + 1)}\right](\mu_G - \mu_E)^2 \quad (3)$$

In non-hydrogen donating solvents $\bar{\nu}_a - \bar{\nu}_f$ for compounds **14a** and **13a** depends in a linear way upon $f'(\varepsilon_r,n)$ with a correlation coefficient of 0.970 and 0.980, respectively. The slope amounts to -9690 ± 810 cm^{-1} and to -15600 ± 1210 cm^{-1} for **14a** and **13a**, respectively. To calculate the difference between the excited state and ground state dipole moment from the slope requires a value for ρ, the cavity radius. This is not straightforward for nonspherical molecules. For molecules as **14a** and **13a**, which can be considered as an ellipsoid, often a value of 40% of the long axis is used. This long axis amounts to 1.37 and 2.00 nm for **14a** and **13a**, respectively. In these cases one obtains values of 14 ± 1 and 30 ± 2 D for the difference between the dipole moments in the excited state and in the ground state of **14a** and **13a**, respectively.

Although the emission maximum exhibits a large red shift upon increasing ε_r, this is not observed for the absorption maximum. This suggests that μ_G is much smaller than μ_E. Under these conditions eqn. (1) can be simplified to eqn. (4):

$$\bar{\nu}_f - \bar{\nu}_f^0 = \frac{2\mu_E^2}{4\pi\varepsilon_0 hc\rho^3} f'(\varepsilon_r, n) \quad (4)$$

with

$$f'(\varepsilon_r, n) = \left[\frac{\varepsilon_r - 1}{2\varepsilon_r + 1} - \frac{n^2 - 1}{2(2n^2 + 1)}\right] \quad (5)$$

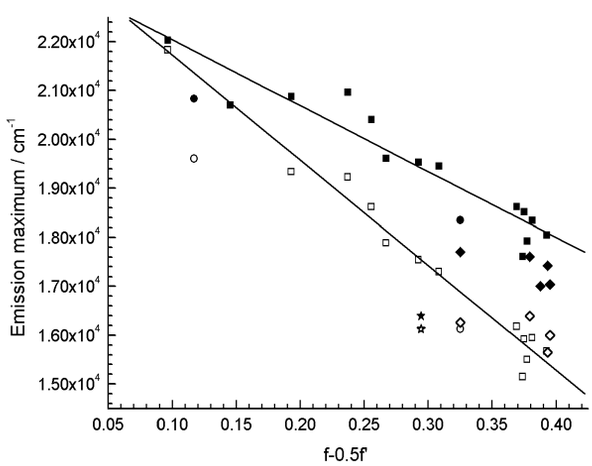

Fig. 5 Dependence of the energy of the fluorescence maximum of **14a** and **13a** upon the solvent polarity parameter $f(\varepsilon_r,n)$ and $f'(\varepsilon_r,n)$; ■: **14a**, aprotic, non-polarizable solvents, ◆: **14a** protic solvents, ●: **14a** polarizable solvents, ★: **14a** acetic acid; □: **13a**, aprotic, non-polarizable solvents, ◇: **13a** protic solvents, ○: **13a** polarizable solvents, ☆: **13a** acetic acid. The lines correspond to a linear least squares fit for the aprotic, non-polarizable solvents.

Fig. 5 shows that in non-hydrogen donating non-polarizable solvents $\bar{\nu}_f$ for compounds **14a** and **13a** depends in a linear way upon $f'(\varepsilon_r,n)$ with a correlation coefficient of 0.952 and 0.987, respectively. The slope amounts to -13470 ± 1250 and -21420 ± 1080 cm^{-1} for **14a** and **13a**, respectively. Using the assumptions made to determine the difference between the dipole moment in the ground state and in the excited state one obtains a dipole moment of 16 ± 1 and 35 ± 2 D for the singlet excited state of **14a** and **13a**, respectively. The estimated error in μ_E is based on the linear regression of $\bar{\nu}_f$ *versus* $f'(\varepsilon_r,n)$ and does not take into account systematic errors related *e.g.* to a non-spherical solvent cavity, the break-down of the point-dipole approximation or the different electronic polarizability of the ground and excited state of **13a** or **14a**.[10]

The data points related to toluene and pyridine are located to the same extent below the linear correlation. This is due to the fact that interactions with aromatic solvents are not only limited to dipole–dipole and dipole–induced dipole interactions, as Van der Waals interactions, charge transfer interactions and dipole–quadrupole interactions can no longer be neglected.[10,39] Also the red shift of the absorption spectra in the relatively nonpolar toluene can be attributed to such Van der Waals interactions and charge transfer interactions.[40] The proton-accepting character of pyridine does not lead to any extra spectral shift.

In ethanol and methanol (Table 2) and to an even larger extent in acetic acid a red shift of the fluorescence maximum is observed compared to the data in aprotic solvents (Figs. 5 and 6)

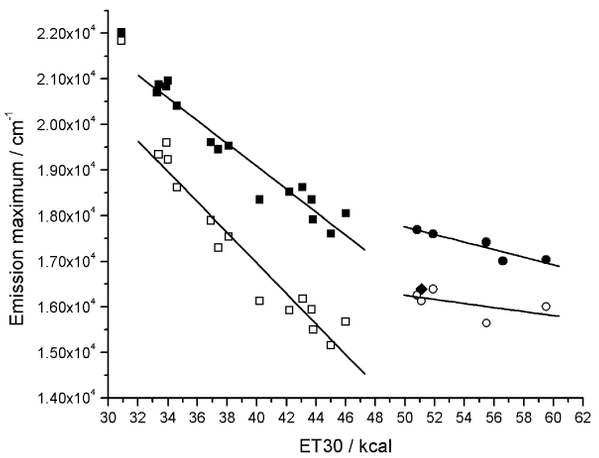

Fig. 6 Dependence of the energy of the fluorescence maximum of **14a** and **13a** upon the solvent polarity parameter ET_{30}; ■: **14a**, aprotic, non-polarizable solvents, ●: **14a** protic solvents, ◆: **14a** acetic acid; □: **13a**, aprotic, non-polarizable solvents, ○: **13a** protic solvents.

for **14a**. For **13a** this red shift is limited to acetic acid. In contrast to the other protic solvents the absorption maximum for both **13a** and **14a** shifts furthermore to 485 nm in acetic acid. This red shift is attributed to protonation of **13a** and **14a**. For **14a** a band attributed to the unprotonated form and absorbing at 430 nm is also observed. The maximum at 430 nm is not due to a dimer as both a solution with an absorbance of 2.59 and of 0.066 at 485 nm showed the same ratio for the absorbances at both maxima. This suggests that the ground state **14a** is more difficult to protonate than that of **13a**. In acetic acid the Stokes shift decreases from 7300 to 3850 cm^{-1} and from 8610 to 4520 cm^{-1} compared to that of the unprotonated form for **14a** and **13a**, respectively. This means that, to the extent that the geometrical relaxation is the same, the charge redistribution becomes less important upon protonation.

As the emission maximum of **13a** and **14a** depends upon the proton donor as well as upon the dipolar character of the solvent we attempted to plot the emission maximum *versus* the empirical parameter ET_{30},[41,42] which takes into account both aspects of solvation. Although ET_{30} is based on the absorption spectra of a molecule with a large ground state dipole moment and a small excited state dipole moment, it can also be used for molecules with a large excited state dipole moment and a small ground state dipole moment. The plot of the emission maxima [$\bar{\nu}_{max}^{f}$ of **14a** (in kcal mol^{-1}) *versus* ET_{30},Fig. 6] suggested two different linear relationships with a slope of -0.72 ± 0.05 and of -0.24 ± 0.06 for the aprotic (without isooctane) and the protic (without acetic acid) solvents, respectively. The correlation coefficients were 0.97 and 0.92, respectively. For compound **13a** the slope and correlation coefficient amounted to -0.96 ± 0.07 and 0.97 or -0.13 ± 0.10 and 0.58 in aprotic and protic solvents, respectively. While for **13a** the data point related to acetic acid could be correlated with those obtained in other protic solvents it was situated at considerably lower energy for **14a**. To obtain a good fit for both **13a** and **14a** the data points in isooctane had to be discarded. This could be due to the fact that in this solvent, where some vibrational fine structure can be observed, the maximum of the emission spectrum corresponds with that of the 0–0 transition rather than with the first moment of the spectrum.

In trifluoroethanol on the other hand a blue shift of the absorption maximum to 379 and 385 nm is observed for **13a** and **14a**, respectively.

To combine the data in protic and aprotic solvents in a single analysis the fluorescence maxima were correlated with the π^* and α-parameter of Taft[14–17,43,44] using multiple linear regression. As **13a** and **14a** have no proton-donating sites no correlation with the proton-acceptor capacity of the solvent, β, was considered.

$$\bar{\nu}_{em} = \bar{\nu}_0 + s\pi^* + a\alpha \qquad (6)$$

When the data point related to toluene, which was situated at too large energies, was discarded the correlation coefficients improved from 0.912 and 0.952 to 0.942 and 0.968 for **13a** and **14a**, respectively. The slope *versus* π^* gave -5550 ± 530 and -3770 ± 320 cm^{-1} for **13a** and **14a**, respectively while the slope *versus* α amounted to -700 ± 320 and -1640 ± 210 cm^{-1} for **13a** and **14a**, respectively. This confirms the different dependence on $f'(\varepsilon_r,n)$ observed in the Lippert–Mataga plots.

Consecutive fluorescence spectra of **13a** and **14a** in toluene and acetic acid were identical and showed no loss of intensity. This indicates that neither the unprotonated nor the protonated (*vide infra*) form of the probes are susceptible to important photodegradation or photo-isomerization.

As proton-accepting solvents apparently influence the absorption and fluorescence spectra of **14a** and **13a** a more comprehensive investigation of this effect was done in methanol.

Halochromism of 14a and 13a in methanol. As the excited state behavior of **14a** and **13a** depends not only upon the solvent dipole moment but also upon its proton-donating character, the effect of the presence of acetic acid (HOAc) and toluene-*p*-sulfonic acid (PTSA) on the spectroscopic properties of **14a** and **13a** will be investigated in more detail in methanol.

For **14a** addition of 0.42 M HOAc to methanol does not lead to a change of the absorption maximum (Table 3), but at the long wavelength side of the spectrum a shoulder appears close to 495 nm (Fig. 7), close to the absorption maximum in acetic acid (Fig. 1). No significant changes in the emission spectrum and fluorescence quantum yield are observed (Fig. 7).

Upon addition of 0.175 M PTSA the absorption spectrum

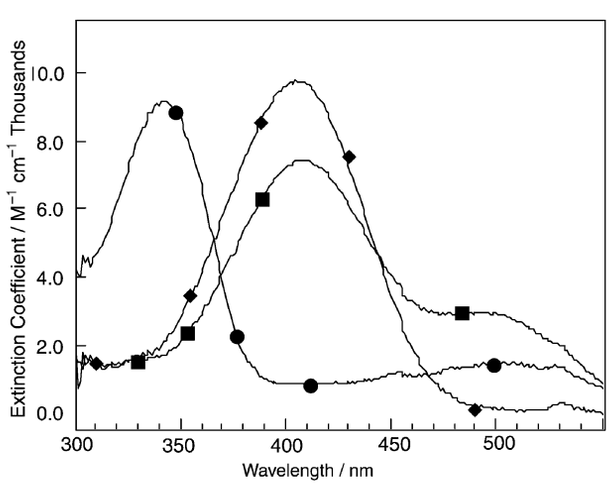

Fig. 7 Absorption spectra of a 4.1×10^{-5} M solution of **14a** in methanol; ◆: no additives, ■: with 0.42 M acetic acid, ●: with 0.175 M toluene-*p*-sulfonic acid. 1.06×10^{-3} M.

Table 3 Halochromism of **14a** and **13a** in methanol

Solvent	**14a**			**13a**		
	$\bar{\nu}_{max}^{abs}$ [a]/nm	$\bar{\nu}_{max}^{flu}$ [b]/nm	φ_f	$\bar{\nu}_{max}^{abs}$ [a]/nm	$\bar{\nu}_{max}^{flu}$ [b]/nm	φ_f
Methanol	406	579	0.23 ± 0.05	411	639	0.043 ± 0.009
Methanol + 0.175 M PTSA [c]	343 (500)	423	0.0035 ± 0.001 [a]	378 (503)	476	0.20 ± 0.04 [b]
Methanol + acetic acid [d]	407 (495)	577	0.16 ± 0.03	(334) 485	631	0.037 ± 0.007
Methanol + buffer 1 [e]	406	581	0.14 ± 0.03	411	639	0.045 ± 0.009
Methanol + buffer 2 [f]	407	581	0.15 ± 0.03	411	639	0.026 ± 0.005
Methanol + buffer 3 [g]	408	581	0.15 ± 0.03	411	639	0.042 ± 0.008
Methanol + CH_3COONa [h]	407	581	0.20 ± 0.03	411	639	0.039 ± 0.008
Methanol + Et_3N [i]	406	581	0.16 ± 0.03	408	639	0.056 ± 0.012

[a] Absorption maximum. [b] Emission maximum. [c] 0.175 M toluene-*p*-sulfonic acid (PTSA). [d] 0.42 M CH_3COOH. [e] 0.267 M CH_3COOH and 0.05 M $CH_3COONa{\cdot}3H_2O$. [f] 0.16 M CH_3COOH and 0.21 M $CH_3COONa{\cdot}3H_2O$. [g] 0.053 M CH_3COOH and 0.625 M $CH_3COONa{\cdot}3H_2O$. [h] 0.420 M $CH_3COONa{\cdot}3H_2O$. [i] 0.19M Et_3N.

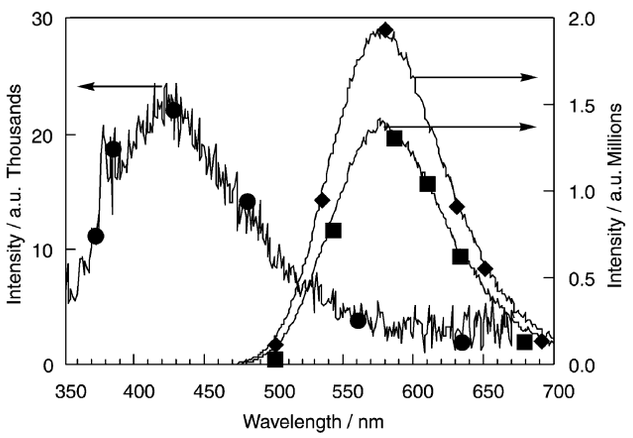

Fig. 8 Fluorescence spectra of a 4.1×10^{-5} M solution of **14a** in methanol normalized to equal light absorption; ◆: no additives, ■: with 0.42 M acetic acid, ●: with 0.17 M toluene-*p*-sulfonic acid. Excitation occurred at 400 nm.

shifts to shorter wavelengths (maximum at 340 nm) (Table 3) with a very small shoulder at 503 nm, while the fluorescence maximum shifts to 430 nm (Fig. 8). This is accompanied by a strong decrease of the fluorescence quantum yield. All three forms (unprotonated, monoprotonated and diprotonated) have a similar molar absorption coefficient.

For **13a** addition of 0.42 M HOAc to methanol shifts the absorption maximum to 485 nm (Fig. 9), which is close to the

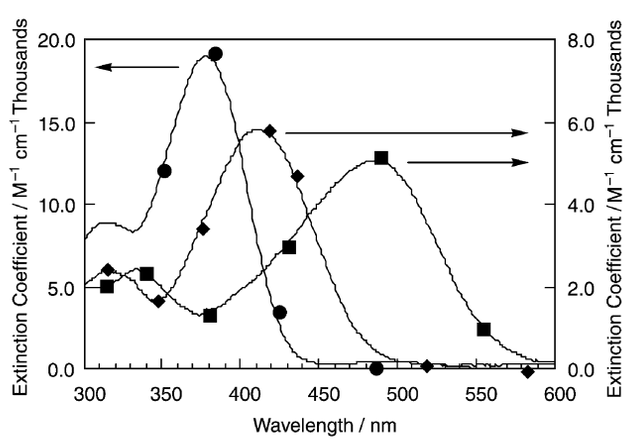

Fig. 9 Absorption spectra of a 2.2×10^{-5} M solution of **13a** in methanol; ◆: no additives, ■: with 0.42 M acetic acid, ●: with 0.175 M toluene-*p*-sulfonic acid.

absorption maximum observed in acetic acid (Fig. 3). No significant changes of the emission spectrum maximum and fluorescence quantum yield are observed. However, the width of the fluorescence spectrum is smaller than those observed for other solvents in which a similar fluorescence maximum is observed. Upon addition of 0.175 M PTSA the absorption spectrum shifts to shorter wavelengths (maximum at 378 nm) with a very small shoulder at 503 nm, while the fluorescence maximum shifts to 476 nm (Fig. 10). This is accompanied by a fivefold

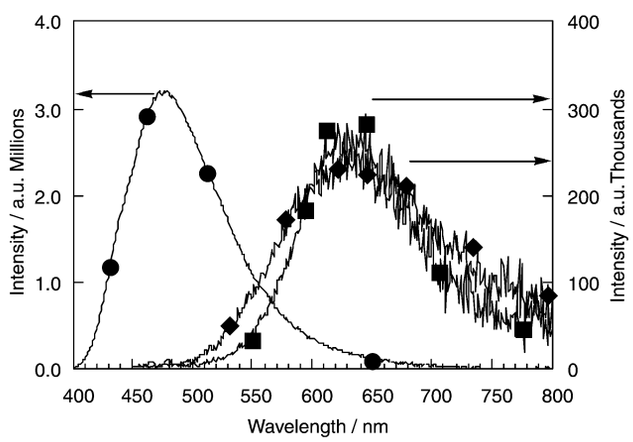

Fig. 10 Fluorescence spectra of a 2.2×10^{-5} M solution **13a** in methanol normalized to equal light absorption; ◆: no additives, ■: with 0.42 M acetic acid, ●: with 0.175 M toluene-*p*-sulfonic acid. Excitation occurred at 410 nm (no additives and with 0.42 M CH_3COOH) and 380 nm (with 0.175 M toluene-*p*-sulfonic acid).

increase of the fluorescence quantum yield. While the ground state species in the absence and presence of HOAc have similar molar absorption coefficients, the species formed in the presence of PTSA has an absorption coefficient that is three times larger.

For both **14a** and **13a** addition of buffers of acetic acid and sodium acetate in a ratio varying between 1 : 10 to 10 : 1 influences neither the absorption nor the emission spectra or the fluorescence quantum yield. Addition of proton acceptors such as *e.g.* sodium acetate or triethylamine has also no influence on the spectral and photophysical properties.

Discussion: photophysical properties

In aprotic solvents

In nonpolar solvents the fluorescence maximum of **13a** is only shifted by 30 nm to longer wavelengths compared to that of **14a**, indicating only a minor stabilization of the excited state due to extension of the conjugation chain. This indicates that **14a** and **13a** are polyenes rather than polymethines in which extending the conjugation chain by an extra vinylene moiety shifts the absorption maximum by 100 nm to longer wavelengths.[45,46,48] Hence, as already inferred from the solvent

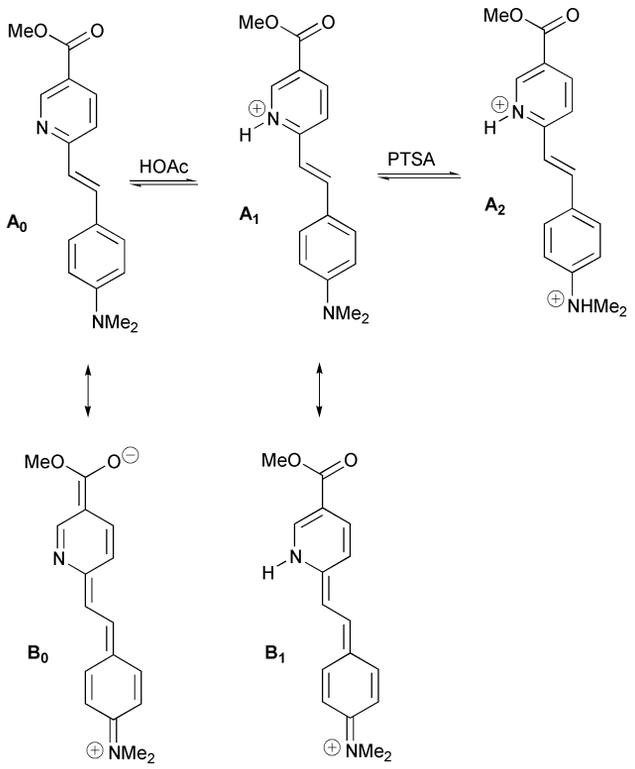

Scheme 3

dependence of the absorption and emission spectrum only a single resonance form $\mathbf{A_0}$ contributes significantly to the ground state (Scheme 3).

In aprotic solvents the solvent dependence of the absorption and fluorescence maxima of **14a** and **13a** can be described in the framework of the Lippert–Mataga equation with a very small ground state dipole moment and a large excited state dipole moment. This can be rationalized in terms of the resonance forms on the left-hand side of Schemes 3 and 4.[11,13,15,17,45–48] In the ground state the aromatic uncharged resonance form $\mathbf{A_0}$ is the major contributor, while in the excited state the dipolar quinoid resonance forms $\mathbf{B_0}$ and $\mathbf{C_0}$ make a major contribution. The linearity of the Lippert–Mataga plot suggests that the excited state electronic structure, which can be visualized as a sum of the contributions of several resonance forms, does not change over the polarity range investigated. The estimated dipole moment of **13a** is considerably larger than that of **14a**.

The fluorescence quantum yield shows different solvent dependences for **14a** and **13a**. For **14a** it increases upon increasing the solvent polarity. Such behavior is characteristic of donor–acceptor substituted stilbenes and has been attributed to the formation of a twisted intramolecular charge transfer state (TICT).[29,49–52] For **13a** it decreases from about 0.25 in solvents of medium polarity to 0.08 in acetonitrile and 0.04 in methanol. This behavior which is sometimes found for cyanine dyes[53–64] is more difficult to rationalize unless further information is available on the relative importance of different non-radiative decay processes (intersystem crossing, isomerization, internal conversion).

In protic solvents

The dependence of the emission spectra of **14a** on the proton donor properties of the solvent, indicated by the fit to the Taft relationship, suggests that in the relaxed excited state a hydrogen bond forms between the pyridine nitrogen and the solvent, which stabilizes the excited state, leading to a red shift of the emission spectrum. As no shift of the absorption maximum is observed, the hydrogen bond will be weak or absent in the ground state. In acetic acid and a 0.42 M solution of acetic acid

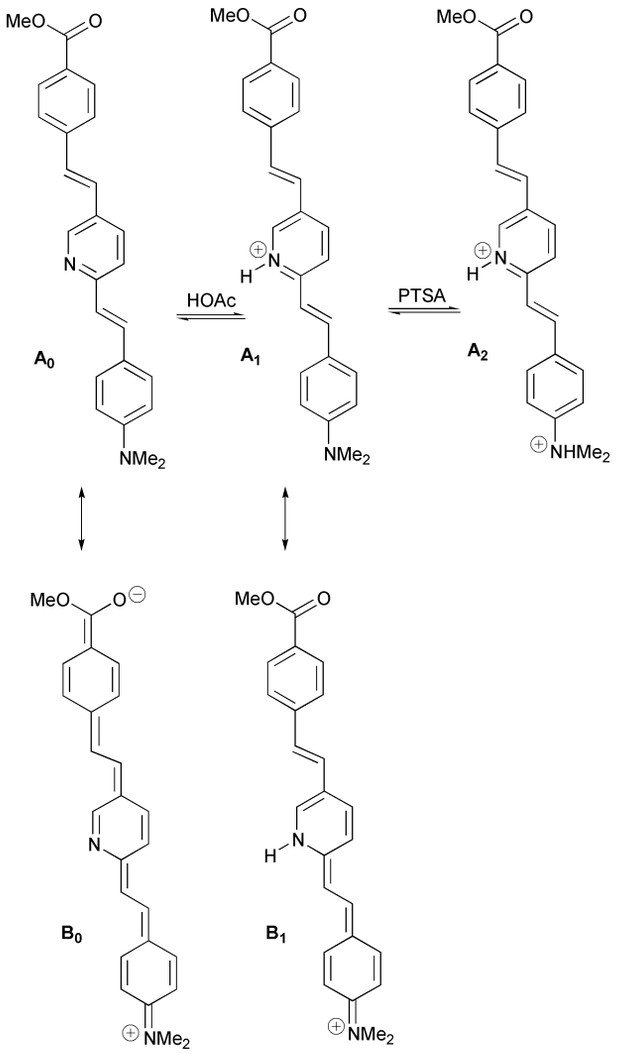

Scheme 4

in methanol a further red shift of the absorption spectrum of **14a** is observed. This indicates that under these conditions the hydrogen bond evolves in a complete proton transfer to the pyridine nitrogen. The persistence of the absorption band at 430 nm for **14a** suggests that in the ground state the protonated species is in equilibrium with the unprotonated one. In undiluted acetic acid this is accompanied by a larger red shift of the emission spectrum compared to the proton-donating solvents, indicating that the emission is completely due to the monoprotonated form. The absence of excited state protonation in a methanol solution with 0.42 M acetic acid indicates however that upon excitation no important decrease in pK_a occurs.

For **13a** the negligible slope of the emission maximum *versus* ET_{30} in proton-donating solvents, which in these solvents is mainly governed by the proton-donor capacity, indicates that no important hydrogen bond formation (with the pyridine nitrogen) occurs upon excitation. Although the absorption spectrum of **13a** indicates protonation of the pyridine nitrogen in the presence of acetic acid and even diprotonation in trifluoroethanol, no indication of excited state protonation or even hydrogen bond formation is observed from the emission spectra. Both the Lippert–Mataga plot[37,38] and the Taft[14–17,43,44] equation indicate that even in acetic acid or trifluoroethanol the emission maximum is determined only by the dipolar properties of solvent [$f(\varepsilon_r,n)$ or π^*]. In toluene-*p*-sulfonic acid both the aniline and pyridine nitrogen become protonated. Of course it remains possible that the emission maximum of a protonated form of **13a** (the emission maximum of which depends by analogy to the hemicyanines and merostyryls only to a limited

extent upon the solvent polarity) is situated in the same wavelength range as that of the unprotonated species in polar solvents. The smaller width of the emission spectrum in acetic acid could support this argument (Fig. 2).

The absorption maximum of the diprotonated form of **13a** and **14a** is situated only at 20 to 30 nm longer wavelengths than of the iso-electronic *trans*-stilbene[65–69] and 1,4-bis(*p*-phenylenevinylene)benzene[70] which are characterized by maxima at 343 and 310 nm, respectively. Also, the emission maximum of the diprotonated **13a** is shifted by about the same energy compared to that of the corresponding energy of 1,4-bis(*p*-phenylenevinylene)benzene with an emission maximum at 431 nm.[71] For **14a** the double protonation reduces the fluorescence quantum yield by a factor of fifty. The extremely low quantum yield of the diprotonated form suggests that its photophysical properties resemble those of stilbazolium salts in low viscosity solvents,[3] in which the excited state rotation around the double bond to a phantom singlet state leads to efficient deactivation. For the diprotonated **13a** on the other hand a much higher fluorescent quantum yield comparable to oligophenylene vinylenes is observed.[72–74]

Although in undiluted acetic acid the absorption maxima of both the protonated and unprotonated form of **14a** are observed, the maximum of the unprotonated **13a** can no longer be observed. In methanol with 0.42 M acetic acid the absorption band of the unprotonated form dominates for **14a** over that of the unprotonated from while for **13a** the absorption bands of the monoprotonated and, to a minor extent, of the diprotonated form are observed. This indicates that the basicity of the pyridine nitrogen is smaller in **14a**, probably due to the proximity of the electron-withdrawing carboxy moiety.

Comparison with other probes

Although the emission spectra of **13a** and **14a** in aprotic solvents show a similar solvent dependence to the absorption maxima of ET_{30},[41,42] they depend much less upon the proton-donor character of the solvent as indicated by Fig. 6. However, in contrast to ET_{30}, which is an absorption probe, **13a** and **14a** are fluorescence probes. The latter allows a much larger sensitivity, needing a much smaller local concentration of the probe. A good fluorescent polarity probe[1–16] should show a large fluorescence shift as a function of the solvent dipole moment and/or hydrogen bond donating or accepting character, absorb at long wavelengths and have a high fluorescent quantum yield.

In aprotic media the dependence of the emission maximum of **14a** and, *a fortiori*, **13a** upon the relative permittivity of the solvent is larger than those of 4-amino-7-nitro-benz-2-oxa-1,3-diazole (NBD),[75] 3-aminophthalimide,[76–78] styrylpyridiniums,[79] quaternized 4-dialkylamino-4′-azastilbenes,[5] 4′-hydroxystyryldiazines[4] or merostyryls[12] and some merocyanines.[11,13,80] They show similar (**13a**) or somewhat larger (**14a**) shifts to ANS[81–84] and related molecules,[85–86] 6-propionyl-2-(dimethylamino)-naphthalene (PRODAN),[87] 6-acryloyl-2-(dimethylamino)-naphthalene (ACRYLODAN)[88] and related molecules,[89] 4-aminophthalimide,[76–78,90–93] hemicyanines,[6,7] aminonitrostilbenes,[94] 4-dimethylamino-4′-(1-oxobutyl)stilbene[95,96] or some other merocyanines[11,13,80] developed by Wolfbeis.[8] In contrast to most other polarity probes and by analogy to hemicyanines[6,7] or quaternized 4-dialkylamino-4′-azastilbenes,[5] the fluorescence maximum of **13a** is not influenced by the hydrogen bond donating character of the solvent. The dependence of the fluorescence maximum of **14a** upon the hydrogen bond donating character of the solvent resembles that of a large number of probes but is smaller than that of 4-aminophthalimide,[75–78,90–93] PRODAN,[87] ACRYLODAN[88] and related molecules[89] or 4-dimethylamino-4′-(1-oxobutyl)stilbene.[95,96]

Although the fluorescence quantum yield of **13a** in polar solvents is smaller than that of PRODAN[87] or ACRYLODAN[88] it at least matches those of the other probes discussed above. In polar solvents it is several orders of magnitude larger than those of the red-absorbing (*cf. infra*) hemicyanines[6,7] or aminonitrostilbenes.[94] In low and medium polarity solvents the fluorescence quantum yields of **13a** are close to those of hemicyanines while those of **14a** are up to one order of magnitude smaller. The fluorescence quantum yield of **14a** in polar solvents matches that of PRODAN[87] or ACRYLODAN[88] and is at least one order of magnitude larger than those of the other probes mentioned above. The similar fluorescence quantum yield observed for **14a** and **13a** (Table 2) in methanol and benzyl alcohol suggests that contrary to what is observed for ANS analogues,[86] this property does not depend upon the solvent viscosity. This confirms the experiments suggesting that photoisomerization is not an important decay channel of the singlet excited state.

Both **14a** and **13a** absorb at wavelengths up to 420 nm, which increases their possible use in a fluorescence microscope. Furthermore, their absorption wavelength is at longer wavelengths than several molecules (aromatic amino acids, NADH) that contribute to the auto-fluorescence of cells. The absorption maxima of the neutral **14a** and **13a** are shifted by 30 to 60 nm to longer wavelengths compared to those of the neutral 3′-hydroxystyryldiazines,[4] 4-dimethylamino-4′-(1-oxobutyl)-stilbene,[95,96] ANS,[81–84] PRODAN[87] or ACRYLODAN[88] or 3- and 4-aminophthalimide.[75–78,90–93] They are blue-shifted by 20 to 40 nm compared to hemicyanines,[6,7] NBD,[75] and aminonitrostilbenes.[94] Compared to the quaternized dialkylamino-4′-azastilbenes,[5] stryrylpyridiniums,[79] or some merocyanines[8,11,13,80] they are blue-shifted by 60 nm to 140 nm in medium polarity solvents. In contrast to the quaternized 4-dialkyamino-4′-azastilbenes,[5] hemicyanines[6,7] or some merocyanines[11,13,80] (which are characterized by a blue shift of the absorption spectrum upon increasing the solvent polarity) or NBD,[75] aminonitrostilbenes[94] or other merocyanines[8] (which are characterized by a red shift of the absorption spectrum upon increasing the solvent polarity), the absorption spectra of **13a** and **14a** do not depend upon the solvent polarity. By analogy to other probes,[5,6,7] for which this information was available, the absorption maxima of **13a** and **14a** are not influenced by the hydrogen bond donating character of the solvent. In this respect they differ from the merosyryls,[12] and some merocyanines[11,13,80] showing a blue shift or from aminonitrostilbenes[94] or other merocyanines[8] showing a red shift in proton-donating solvents. This means that for **14a** and **13a** excitation will occur with the same efficiency independently of the solvent polarity.

By analogy to 4′-hydroxystyryldiazines[4] the absorption maxima of **13a** and **14a** shift to considerably lower energy upon protonation. The red shift of the emission maximum upon hydrogen bond formation or protonation of **14a** resembles that of the 4′-hydroxystyryldiazines for which protonation and hydrogen bond formation also induce a red shift (with exception of the 2,4-diazine).[4] The protonated **14a** and **13a** would have a more appropriate excitation wavelength than the unprotonated form. However, as the formation of a protonated **14a** and **13a** requires the addition of acid to the solvent, which will also change the polarity of the cybotactic zone, straightforward study of the influence of the solvent polarity upon the absorption and fluorescence properties would become highly complicated under such conditions. Furthermore, when **14a** and **13a** are used under physiological conditions they will probably be present in the neutral form. Although the emission spectra of the merostyryls[12] are essentially pH dependent, this effect occurs at high pH, while **14a** and **13a** show a pH dependence at low pH or no pH dependence, respectively. In the latter aspect **14a** and **13a** also differ also from carboxy substituted cyanines.[9]

Conclusions

Although proton activity in water and methanol cannot be compared directly, the results obtained in methanol suggest

that, except in a clearly acidic solution, no protonation of **14a** and **13a** is expected in the ground state in an aqueous medium. The similar fluorescent properties of the excited state of the protonated and unprotonated molecules in methanol or trifluoroethanol suggest that under these conditions the protonation does not persist after excitation for **13a** or that the emission spectrum of the protonated form resembles that of the unprotonated form in highly polar solvents.

In aprotic media the solvent dependence of the fluorescence maxima of the unprotonated **14a** and **13a** depends in a linear way upon the Bayliss parameter $f'(\varepsilon_r,n)$, ET_{30} and the Taft parameter π^*. Whereas proton-donating solvents such as ethanol and methanol shift the fluorescence maximum of **14a** to longer wavelengths this effect is not observed for **13a**. This is confirmed by multiple linear regression in the framework of the Taft equation. Hence, the energy of the fluorescence maximum of **13a** allows one to estimate the presence of dipolar molecules in the environment, correlated to ε_r, or the π^* parameter, directly. On the other hand, in proton-donating solvents the emission of **14a** is shifted to longer wavelengths compared to the energy predicted by the Lippert–Mataga equation [eqns. (4) and (5)]. This is indicated by the large *a* parameter found for compound **14a** in the Taft equation [eqn. (6)]. When the fluorescence maximum of **14a** indicates an apparently higher polarity (ε_r) than **13a** the occurrence of hydrogen bonding by a hydrogen donating environment should be considered.

Both **14a** and **13a** absorb at wavelengths up to 420 nm, which increases their possible use in a fluorescence microscope. Furthermore, their absorption wavelength is at longer wavelengths than several molecules (aromatic amino acids, NADH) that contribute to the auto-fluorescence of cells. To the extent that excitation at 400 or 410 nm is no major problem the probes **14a** and **13a** are comparable to or better than several others from the point of view of sensitivity and fluorescence quantum yield, especially if a "selective" probing of the static polarisability (relative permittivity) is envisaged. When interference with the auto-fluorescence of species absorbing above 400 nm is a problem the red-shifted absorption makes the quaternized azastilbenes,[5] NBD[75] or styrylpyridiniums[79] clearly superior, in spite of their smaller solvent dependence of the emission maximum and the solvent dependence of their absorption spectra. Combining both probes **13a** and **14a** will give a simultaneous indication of the static relative permittivity and the proton-donating properties of the medium. Furthermore, their synthesis facilitates easy optimization of their chemical structure, allowing one to optimize, for example, their hydrophobic and membrane-binding properties by attachment of hydrophobic moieties at several substitution positions. The latter will allow one to optimize the probes for inter- or intra-cellular use. Such groups can be incorporated by adapting the aldehydes used for Wittig olefination or for Knoevenagel condensation. Alternatively, when using oxazinones as the starting materials, various substituents could also be introduced into the central core unit.

Experimental

Synthesis

NMR spectra were recorded on a Bruker WM250 or a Bruker AMX 400 instrument. *J* values are given in Hz. IR spectra were recorded on a Perkin-Elmer 1720 Infrared Fourier Transform Spectrometer. Mass spectra were recorded on a Kratos MS50 (ionization energy 70 eV) instrument and DS90 data system. The ion source temperature was 150–250 °C, as required. Exact mass measurements were performed at a resolution of 10000. Elemental analysis was performed by Janssen Pharmaceutica on a Carlo Erba elemental analyzer type 1106. All melting points are uncorrected. Analytical thin layer plates (Sil G/UV 254) and silica gel (70–230 mesh) for column chromatography from Macherey-Nagel or Fluka were used. Aluminium oxide 507 C neutral from Fluka, deactivated with water (6 g per 100 g), was used for column chromatography. Further synthetic details are available as electronic supplementary information (ESI). †

Spectroscopy

The absorption spectra were recorded with a DW-2000 Aminco or a Perkin Elmer Lamda 6 spectrophotometer. The fluorescence and excitation spectra were determined on a SPEX Fluorolog in a rectangular configuration. The spectra were obtained in S/R (sample over reference) mode and corrected for the wavelength dependence of the detection. The fluorescence quantum yields were determined *versus* a degassed solution of 9-cyanoanthracene in methanol (excitation at 420 nm, φ_f = 0.87)[97,98] and *versus* a solution of diphenyloxazole (POPOP) in methanol (excitation at 340 and 380 nm, φ_f = 0.91).[99,100] As a fluorescence decay time below 5 ns was expected for the stilbazole derivatives, the solutions were not degassed. For the halochromic experiments all solutions were prepared from a stock solution of the dye in acetonitrile and the spectra were determined within 2 hours of preparation. For all the fluorescence spectra the absorbance at the excitation wavelength (close the maximum of the absorption spectrum) was always less than 0.1 in a 1 cm cell. Taking into account a molar absorption coefficient of at least 10^4 M^{-1} cm^{-1}, this corresponds to a concentration of 1.0×10^{-5} M or lower.

Acknowledgements

W.V. acknowledges the IWT for a scholarship. The authors gratefully acknowledge the F.K.F.O., the "Nationale Loterij", the research council of K.U. Leuven through G.O.A 1996 and G.O.A. 2001/2 and the continuing support from DWTC (Belgium) through IUAP IV-11 and IUAP V-03.

References

1 J. R. Lakowicz, in *Principles of Fluorescence and Spectroscopy*, Plenum Press, New York, 1983.
2 A. C. Stevens, R. P. Frutos, D. F. Harvey and A. A. Brian, *Bioconjugate Chem.*, 1993, **4**, 19.
3 S. Sharafy and K. A. Muszkat, *J. Am. Chem. Soc.*, 1971, **93**, 4119.
4 S. A. Haroutounian and J. A. Katzenellenbogen, *Tetrahedron*, 1995, **51**, 1585.
5 H. Görner and H. Grön, *J. Photochem.*, 1985, **28**, 329.
6 H. Ephardt and P. Fromherz, *J. Phys. Chem.*, 193, **97**, 4540.
7 P. Fromherz, *J. Phys. Chem.*, 1995, **99**, 7188.
8 M. A. Kessler and O. S. Wolfbeis, *Spectrochim. Acta, Part A*, 1991, **47**, 187.
9 A. E. Boyer, S. Devanathan, D. Hamilton and G. Patonay, *Talanta*, 1992, **39**, 505.
10 P. Suppan, *J. Photochem. Photobiol., A*, 1990, **50**, 293.
11 P. Jacques, *J. Phys. Chem.*, 1986, **90**, 5535.
12 M. S. A. Abdel Mottaleb and A. M. K. Sherief, *Z. Phys. Chem. (Leipzig)*, 1984, **265**, 154–160.
13 S. Abdel-Halim and M. K. Awad, *J. Phys. Chem.*, 1993, **97**, 3160.
14 R. W. Taft and M. J. Kamlet, *J. Am. Chem. Soc.*, 1976, **98**, 2886.
15 M. J. Kamlet, J. L. Abboud, M. H. Abraham and R. W. Taft, *J. Org. Chem.*, 1983, **48**, 2877.
16 J.-L. Abboud and R. W. Taft, *J. Phys. Chem.*, 1979, **83**, 412.
17 M. J. Kamlet, J. L. Abboud, M. H. Abraham and R. W. Taft, *J. Am. Chem. Soc.*, 1977, **99**, 6027.
18 D. L. Rousseau, in *Optical Techniques in Biological Research*, Academic Press New York, 1984, ch. 4.
19 See for example: (*a*) L. Meerpoel and G. Hoornaert, *Tetrahedron Lett.*, 1989, **30**, 3183; (*b*) L. Meerpoel and G. Hoornaert, *Synthesis*, 1990, 905; (*c*) L. Meerpoel, S. M. Toppet, F. Compernolle and G. J. Hoornaert, *Tetrahedron*, 1991, **47**, 10065; (*d*) L. Meerpoel, G. Deroover, K. Van Aken, G. Lux and G. Hoornaert, *Synthesis*, 1991, 765; (*e*) L. Meerpoel, G. J. Joly and G. Hoornaert, *Tetrahedron*, 1993, **49**, 4085; (*f*) B. Medaer, K. Van Aken and G. Hoornaert, *Tetrahedron Lett.*, 1994, **35**, 9767; (*g*) K. J. Van Aken, G. M. Lux, G. G. Deroover, L. Meerpoel and G. J. Hoornaert,

Tetrahedron, 1994, **50**, 5211; (*h*) P. R. Carly, F. Compernolle and G. J. Hoornaert, *Tetrahedron Lett.*, 1995, **36**, 2113; (*i*) P. R. Carly, S. L. Cappelle, F. Compernolle and G. J. Hoornaert, *Tetrahedron*, 1996, **52**, 11889; (*j*) B. P. Medaer, K. J. Van Aken and G. J. Hoornaert, *Tetrahedron*, 1996, **52**, 8813; (*k*) N. Knoops, G. Deroover, Z. Jidong, F. Compernolle and G. J. Hoornaert, *Tetrahedron*, 1997, **53**, 12699; (*l*) E. Van der Eycken, G. Deroover, S. M. Toppet and G. J. Hoornaert, *Tetrahedron Lett.*, 1999, **40**, 9147 and references cited therein.
20 K. J. Van Aken, G. M. Lux, G. G. Deroover, L. Meerpoel and G. J. Hoornaert, *Tetrahedron*, 1994, **50**, 5211.
21 M. Freifelder, *Practical Catalytic Hydrogenation*, Wiley, New York, 1971, p. 447.
22 J. N. Pattison and E. Degering, *J. Am. Chem. Soc.*, 1951, **73**, 611.
23 C. W. Whitehead, J. J. Traverso, F. J. Marshall and P. E. Morrison, *J. Org. Chem.*, 1961, **26**, 2809.
24 M. Hasegawa, *Pharm. Bull. Jpn.*, 1953, **1**, 293.
25 J. P. Kutney, W. Cretney, T. Tabata and M. Frank, *Can. J. Chem.*, 1964, **42**, 698.
26 S. S. Kim, S. Y. Choi and C. H. Kang, *J. Am. Chem. Soc.*, 1985, **107**, 4234.
27 I. Gosney, A. G. Rowley, *Organophosphorus Reactions in Organic Synthesis*, Academic Press, New York, 1979; L. D. Bergelson and M. M. Shemyakin, *Pure Appl. Chem.*, 1964, **9**, 271; A. B. Reitz, S. O. Nortey, A. D. Jordom, M. S. Mutter and B. E. Maryanoff, *J. Org. Chem.*, 1986, **51**, 3302.
28 H. H. Jaffé, M. Orchin, in *Theory and Applications of Ultraviolet Spectroscopy*, John Wiley, New York, 1962.
29 W. Rettig and V. Bonačič-Koutecky', *Chem. Phys. Lett.*, 1979, **62**, 115.
30 Z. R. Grabowski, K. Rotkiewicz, A. Siemiarczuk, D. Cowley and J. W. Baumann, *Nouv. J. Chim.*, 1979, **3**, 443.
31 R. W. H. Berry, P. Brocklehurst and A. Burawoy, *Tetrahedron*, 1960, **10**, 109.
32 A. Safarzadeh-Amiri, *Chem. Phys.*, 1988, **125**, 145.
33 L. E. Bolívar, M. C. dos Santos and D. S. Galvaõ, *J. Phys. Chem.*, 1996, **100**, 11029.
34 J. N. Murrell, in *The Theory of Electronic Spectra of Organic Molecules*, J. Wiley & Sons, New York, 1963.
35 H. K. Sinha and K. J. Yates, *J. Am. Chem. Soc.*, 1991, **113**, 6062.
36 T. P. Carsey, G. L. Findley and S. P. Mc Glynn, *J. Am. Chem. Soc.*, 1979, **101**, 4502.
37 E. Lippert, *Z. Naturforsch., A: Astrophys. Phys. Phys. Chem.*, 1955, **10**, 541.
38 N. Mataga, Y. Kaifu and M. Koizumi, *Bull. Chem. Soc. Jpn.*, 1955, **28**, 690.
39 D. Gupta and S. Basu, *J. Photochem.*, 1975, **4**, 307.
40 G. Verbeek, S. Depaemelaere, M. Van der Auweraer, F. C. De Schryver, A. Vaes, D. Terrell and S. De Meutter, *Chem. Phys.*, 1993, **176**, 195.
41 K. Dimroth and C. Reichardt, *Liebigs Ann. Chem.*, 1969, **727**, 93.
42 C. Reichardt, *Angew. Chem.*, 1979, **91**, 119.
43 R. W. Taft and M. J. Kamlet, *J. Chem. Soc., Perkin Trans. 2*, 1979, 1723.
44 M. J. Kamlet, T. N. Hall, J. Boykin and R. W. Taft, *J. Org. Chem.*, 1979, **44**, 2599.
45 L. G. S. Brooker, G. H. Keyes and D. W. Heseltine, *J. Am. Chem. Soc*, 1951, **73**, 5350.
46 L. G. S. Brooker, A. C. Craig, D. W. Heseltine, P. W. Jenkins and L. L. Lincoln, *J. Am. Chem. Soc.*, 1965, **87**, 2443.
47 Th. Förster, *Z. Elektrochem.*, 1969, **45**, 548.
48 W. T. Simpson, *J. Am. Chem. Soc.*, 1951, **73**, 5359.
49 M. Meyer, J.-C. Mialocq and B. Perly, *J. Phys. Chem.*, 1990, **94**, 98.
50 J. F. Létard, R. Lapouyade and W. Retig, *Chem. Phys. Lett.*, 1994, **222**, 209.
51 A. V. Deserpandi, A. Beidoun and A. Penzkofer, *Chem. Phys.*, 1990, **148**, 141.
52 W. Rettig, W. Majenz, R. Lapouyade and G. Hancke, *J. Photochem. Photobiol., A*, 1992, **62**, 415.
53 M. Van der Auweraer, M. Van den Zegel, F. C. De Schryver, N. Boens and F. Willig, *J. Phys. Chem.*, 1986, **90**, 1169.
54 A. S. Tatikolov, R. A. Shredova, N. A. Derevyanko, A. A. Ishenko and V. A. Kuzmin, *Chem. Phys. Lett.*, 1992, **190**, 291.
55 N. Khimenko, A. K. Chibisov and H. Görner, *J. Phys. Chem. A*, 1997, **101**, 7304.
56 D. Pevenage, D. Corens, M. Van der Auweraer and F.-C. De Schryver, *Bull. Soc. Chim. Belg.*, 1997, **106**, 565.
57 S. A. Soper and Q. A. Mattifly, *J. Am. Chem. Soc.*, 1994, **116**, 3744.
58 D. Noukakis, M. Van der Auweraer, S. Toppet and F. C. De Schryver, *J. Phys. Chem.*, 1995, **99**, 11860.
59 S. Murphy and G. B. Schuster, *J. Phys. Chem.*, 1995, **99**, 8516.
60 I. Martini and G. N. Hartland, *Chem. Phys. Lett.*, 1996, **258**, 180.
61 M. R. V. Sahyun and J. T. Blair, *J. Photochem. Photobiol., A*, 1997, **104**, 179.
62 N. Livakumar, E. A. Hoburg and D. H. Waldeck, *J. Chem. Phys.*, 1989, **90**, 2305.
63 E. Laitinen, P. Ruuskanen-Järvinrn, U. Rempel, V. Helenius and J. E. L. Korppi-Tommola, *Chem. Phys. Lett.*, 1994, **218**, 73.
64 M. Krieg and R. W. Redmond, *Photochem. Photobiol.*, 1993, **57**, 472.
65 J. A. Syage, W. R. Lambert, P. M. Pelker and A. H. Zewail, *Chem. Phys. Lett.*, 1982, **88**, 266.
66 J. B. Birks, in *Organic Molecular Photophysics*, ed. J. B. Birks, John Wiley & Sons, London, 1975, vol. 2, p. 441.
67 K. Sandros and M. Sundahl, *J. Phys. Chem.*, 1994, **98**, 5705.
68 H. Hamaguchi and K. Iwata, *Chem. Phys. Lett.*, 1993, **208**, 465.
69 J. Saltiel, S. Waller, D. F. Sears, E. A. Hoburg, D. M. Leglinski and D. H. Waldeck, *J. Phys. Chem.*, 1994, **98**, 10689.
70 Y. Geerts, G. Klärner and H. Müllen, in *Electronic Materials, The Oligomer Approach*, eds. K. Müllen and G. Wegner, Wiley VCH, Weinheim, 1998, p. 69.
71 A. Schmidt, M. L. Anderson, D. Dunphy, Th. Wehrmeister, K. Müllen and N. Armstrong, *Adv. Mater.*, 1995, **7**, 722.
72 P. Van Hutten, V. V. Krasnikov and G. Hadziioannou, *Acc. Chem. Res.*, 1999, **32**, 257.
73 R. E. Gill, A. Hilberer, P. F. Van Hutten, G. Berentschot, M. P. L. Werts, A. Meetsma, J.-C. Wittmann and G. Hadziioannou, *Synth. Met.*, 1997, **84**, 637.
74 C. M. Hiller, I. H. Campbell, B. K. Laurich, D. L. Smith, D. D. C. Bradley, P. L. Burn, J. P. Ferraris and K. Müllen, *Phys. Rev. B*, 1996, **54**, 5516.
75 S. Féry-Forgues, J.-P. Fayet and A. Lopez, *J. Photochem. Photobiol., A*, 1993, **70**, 229.
76 Th. Förster and K. Rokos, *Z. Phys. Chem., Neue Folge*, 1969, **63**, 208.
77 W. R. Ware, S. K. Lee, G. J. Brant and P. P. Chow, *J. Chem. Phys.*, 1971, **54**, 4729.
78 N. G. Bakhshiev, Y. T. Muzurenko and I. V. Piterskaya, *Opt. Spektrosk.*, 1962, **12**, 350 (*Opt. Spectrosc. (Engl. Transl.)*, 1962, **12**, 193).
79 G. Y. Dubur, G. E. Dobretsov, A. K. Deme, R. R. Dubure, E. N. Lapshin and M. M. Spirin, *J. Biochem. Biophys. Methods*, 1984, **10**, 123.
80 S. T. Abdel-Halim, M. Abddel-Kader and U. Steiner, *J. Phys. Chem.*, 1988, **92**, 4324.
81 E. Kosower, *Acc. Chem. Res.*, 1982, **15**, 259.
82 L. Stryer, *J. Mol. Biol.*, 1965, **13**, 483.
83 L. Stryer, *Science*, 1968, **162**, 536.
84 E. Kosower, H. Dodiuk, K. Tanizawa, M. Ottolenghi and N. Orbach, *J. Am. Chem. Soc.*, 1975, **97**, 2167.
85 E. Kosower and H. Kanety, *J. Am. Chem. Soc.*, 1983, **105**, 6236.
86 E. M. Kosower and H. Dodiuk, *J. Am. Chem. Soc.*, 1978, **100**, 4173.
87 G. Weber and F. J. Farris, *Biochemistry*, 1979, **18**, 3075.
88 F. G. Prendergast, M. Meyer, G. L. Carlson, S. Lida and J. D. Potter, *J. Biol. Chem.*, 1983, **258**, 7541.
89 M. I. Sandez, A. Suàrez, M. A. Rios, M. C. Balo, F. Fernàndez and C. Lòpez, *Photochem. Photobiol.*, 1996, **64**, 486.
90 N. G. Bakhshiev, *Opt. Spektrosk.*, 1962, **12**, 557 (*Opt. Spectrosc. (Engl. Transl.)*, 1962, **12**, 309).
91 N. G. Bakhshiev, *Opt. Spektrosk.*, 1962, **13**, 92 (*Opt. Spectrosc. (Engl. Transl.)*, 1962, **13**, 104).
92 T. Veselova, L. A. Limareva and A. S. Cherkasov, *Opt. Spektrosk.*, 1965, **19**, 78 (*Opt. Spectrosc. (Engl. Transl.)*, 1965, **19**, 39).
93 N. G. Bakhshiev, Y. T. Muzurenko and I. V. Piterskaya, *Opt. Spektrosk.*, 1966, **20**, 783 (*Opt. Spectrosc. (Engl. Transl.)*, 1966, **20**, 437).
94 D. M. Shin and D. G. Whitten, *J. Phys. Chem.*, 1988, **92**, 2945.
95 A. Safardazeh-Amiri, *J. Photochem. Photobiol., A*, 1988, **43**, 43.
96 A. Safardazeh-Amiri, M. Thompson and U. J. Krull, *J. Photochem. Photobiol., A*, 1989, **47**, 299.
97 S. L. Murov, I. Carmichael and G. L. Hug, in *Handbook of Photochemistry*, 2nd edn., Marcel Dekker, Inc., New York, 1993, p. 8.
98 W. R. Ware and W. Rothman, *Chem. Phys. Lett.*, 1976, **39**, 449.
99 S. L. Murov, I. Carmichael and G. L. Hug, in *Handbook of Photochemistry*, 2nd edn., Marcel Dekker, Inc., New York, 1993, p. 36.
100 M. Mardelli and J. M. Olmsted III, *J. Photochem.*, 1977, **7**, 277.